# RADIOCARBON – A UNIQUE TRACER OF GLOBAL CARBON CYCLE DYNAMICS

Ingeborg Levin • Vago Hesshaimer

Institut für Umweltphysik, University of Heidelberg, Im Neuenheimer Feld 229, D-69120 Heidelberg, Germany.
Email: Ingeborg.Levin@iup.uni-heidelberg.de.

## INTRODUCTION

Climate on Earth strongly depends on the radiative balance of its atmosphere, and thus, on the abundance of the radiatively active greenhouse gases. Largely due to human activities since the Industrial Revolution, the atmospheric burden of many greenhouse gases has increased dramatically. Direct measurements during the last decades and analysis of ancient air trapped in ice from polar regions allow the quantification of the change in these trace gas concentrations in the atmosphere. From a presumably "undistorted" preindustrial situation several hundred years ago until today, the $CO_2$ mixing ratio increased by almost 30% (Figure 1a) (Neftel et al. 1985; Conway et al. 1994; Etheridge et al. 1996). In the last decades this increase has been nearly exponential, leading to a global mean $CO_2$ mixing ratio of almost 370 ppm at the turn of the millennium (Keeling and Whorf 1999).

The atmospheric abundance of $CO_2$, the main greenhouse gas containing carbon, is strongly controlled by exchange with the organic and inorganic carbon reservoirs. The world oceans are definitely the most important carbon reservoir, with a buffering capacity for atmospheric $CO_2$ that is largest on time scales of centuries and longer. In contrast, the buffering capacity of the terrestrial biosphere is largest on shorter time scales from decades to centuries. Although equally important today, the role of the terrestrial biosphere as a sink of anthropogenic $CO_2$ emissions is still poorly understood. Any prediction of future climate strongly relies on an accurate knowledge of the greenhouse gas concentrations in the present-day atmosphere, and of their development in the future. This implies the need to quantitatively understand their natural geophysical and biochemical cycles including the important perturbations by human impact.

In attempting to disentangle the complexity of these cycles, radiocarbon observations have played a crucial role as an experimental tool enlightening the spatial and temporal variability of carbon sources and sinks. Studies of the "undistorted" natural carbon cycle profit from the radioactive decay of ^{14}C in using it as a dating tracer, e.g. to determine the turnover time of soil organic matter (SOM) or to study internal mixing rates of the global oceans. Moreover, the anthropogenic disturbance of ^{14}C through atmospheric bomb tests has served as an invaluable tracer for gaining insight into the global carbon cycle on the decadal time scale.

### Global Atmospheric Carbon Dioxide Cycle

The mean residence time of carbon dioxide in the atmosphere is in the order of only 5 yr. Accordingly, 20% of the atmospheric $CO_2$ inventory of today about 750 GtC (1 GtC = $10^9$ metric tons of Carbon = $10^{15}$ g C) are annually exchanged with the biosphere (ca. 60 GtC per year) and the ocean surface waters (ca. 90 GtC per year) (Schimel et al. 1995). Compared to this large *gross* exchange of carbon between reservoirs, the total yearly *net* perturbation fluxes are smaller by more than one order of magnitude: In the 1980s, the input of $CO_2$ into the atmosphere from burning of fossil fuels and cement production summed up to about 6 GtC $yr^{-1}$, and, in addition, about 1–2 GtC $yr^{-1}$ was released in the course of deforestation and land use change. Although the effect of these emissions on the atmospheric $CO_2$ concentration is clearly observed and well documented, it adds up to a mean increase of only 3 GtC $yr^{-1}$ in the atmospheric burden during the 1980s (Figure 1a). The remaining fraction, corresponding to about 50% of the fossil fuel emissions, is buffered away about equally by

the world oceans and the biosphere. This partitioning of anthropogenic $CO_2$ between buffer reservoirs is determined by the dynamics of their internal mixing as well as by the strength of their gross carbon exchange with the atmosphere and leads to a residence time of *excess* man-made $CO_2$ in the atmosphere as large as several hundred years. Despite intensive research in the last decades, the uncertainty of the *gross* exchange rates between carbon reservoirs is still in the order of ±20%, and it remains difficult to univocally quantify the repartition of net uptake between the biosphere and the oceans, and thus, to predict the fate of anthropogenic $CO_2$ emissions. The situation is further complicated by the fact that the share of excess $CO_2$ taken up by the biosphere and oceans may clearly change in the near future under possibly changing climatic conditions. This concerns in particular the terrestrial biospheric reservoir, which has only a small carbon inventory (about 2200 GtC) compared with the oceans (39,000 GtC). Moreover, this reservoir consists of living plants and dead SOM, which are highly vulnerable and already today strongly perturbed by human activity.

The terrestrial biosphere shows a large diversity, ranging from high-latitude tundra and boreal forests, to cultivated land and grassland, to equatorial evergreen forests. In the oceans, the repartition of carbon is less heterogeneous but a large temporal and spatial variability of dissolved inorganic carbon (DIC) is still observed. Therefore, reliable uptake rates of excess $CO_2$ resulting from net changes of the carbon inventory in the oceans and in the biosphere are difficult to obtain by *direct* long-term observations in these reservoirs. In contrast, the atmosphere, being well-mixed in comparison to the biosphere and the oceans, is presently the best-known of all carbon reservoirs. Substantial information about the carbon cycle has been derived from the interpretation of the observed spatial and temporal variability of atmospheric $CO_2$ in combination with model simulations of the biosphere and the oceans. Consequently, in the past, net anthropogenic carbon fluxes into the biosphere and oceans have been mainly estimated from the gross exchanges between the atmosphere and these reservoirs, also taking into account their internal dynamics. These models have been constrained by suitable (transient) tracers such as bomb $^{14}C$, tritium, and chlorofluorocarbons in the case of the oceans, and by natural and bomb $^{14}C$ in the case of the biosphere. The most prominent examples of the application of $^{14}C$ will be discussed in the following sections.

**Global $^{14}C$ Suess Effect Derived from Tree-Ring Analyses**

It has been erroneously argued that the observed atmospheric $CO_2$ increase since the middle of the 19th century may be due to an ongoing natural perturbation of gross fluxes between the atmosphere, biosphere, and oceans. That the increase is in fact a predominantly anthropogenic disturbance, caused by accelerated release of $CO_2$ from burning of fossil fuels, has been elegantly demonstrated through $^{14}C$ analyses of tree rings from the last two centuries (Stuiver and Quay 1981; Suess 1955; Tans et al. 1979). Figure 1c shows high-precision $^{14}C$ data mostly from single tree rings of two Douglas-firs grown from 1815 to 1975 at the Olympic Peninsula (48°N, 124°W) about 15 km from the Pacific coast of the United States (Stuiver and Quay 1981). A strong decrease of about $\Delta^{14}C = -20‰$ from 1890 to 1950 is observed in these tree rings. Only a small fraction ($\Delta^{14}C = -3‰$) of this decrease is estimated by Stuiver and Quay to be due to natural processes (namely the changing natural $^{14}C$ production rate through solar and geomagnetic variations), the remaining decrease being attributed to increasing dilution of $^{14}C$ in atmospheric $CO_2$ by input of $^{14}C$-free fossil fuel $CO_2$ (the so-called $^{14}C$ Suess effect). Taking into account the fossil fuel emission rates for the time span in question (Figure 1b) the Suess effect could be quantitatively reproduced by these authors (and independently by Siegenthaler [1983]) using a carbon reservoir box diffusion model. The overwhelming effect of bomb $^{14}C$ on the atmospheric $^{14}C$ level from 1950 onwards, which cancelled out the $^{14}C$ Suess effect from 1955 onwards (shaded area in Figure 1c), is discussed in the next section.
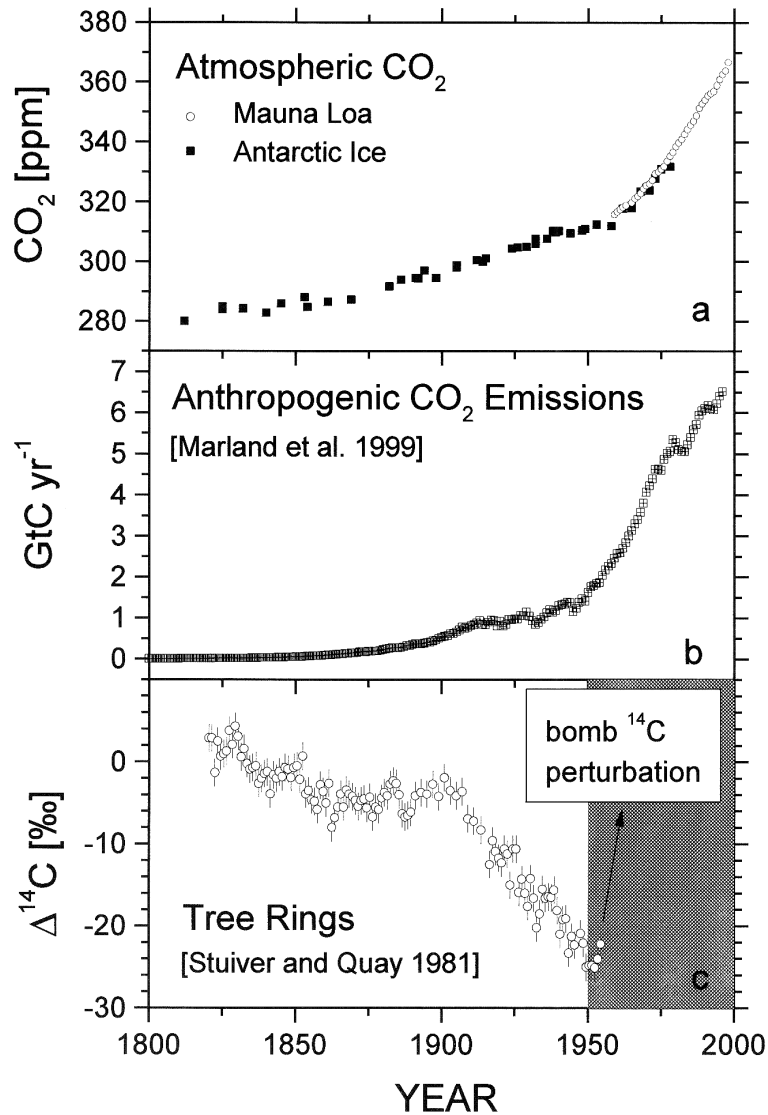
Figure 1 (a) Atmospheric $CO_2$ increase derived from direct observations at Mauna Loa station (Keeling and Whorf 1999) and from analysis of air inclusions in Antarctic ice cores (Etheridge et al. 1996). (b) Anthropogenic $CO_2$ emissions from fossil fuel burning, cement manufacturing and gas flaring. (c) Temporal change of $\Delta^{14}C$ in tree rings grown at the Pacific coast: The $\Delta^{14}C$ decrease is closely related to the increasing anthropogenic $CO_2$ emissions and the resulting increase in atmospheric $CO_2$ mixing ratio. (Note: after 1955 the decreasing $\Delta^{14}C$ trend ends due to the overwhelming effect of bomb $^{14}C$ input into the atmosphere.)

The $\Delta^{14}C$ depletion in the first half of the 20th century has been shown to be larger in more polluted areas, such as Europe, than at the west coast of the United States (De Jong and Mook 1982). In particular, highly populated areas show regional Suess effects up to $\delta\Delta^{14}C = -100‰$, especially during winter (Levin et al. 1989). A discussion of the use of $^{14}C$ for regional studies in the context of verifying emission reductions (as agreed upon in the Kyoto Protocol), will be given below (Regional Suess Effect section).

## Direct Long-Term Observations of Bomb $^{14}CO_2$ in the Global Carbon Reservoirs

During the atmospheric nuclear weapons tests in the 1950s and early 1960s, large amounts of $^{14}C$, in total $630 \times 10^{26}$ atoms of $^{14}C$ or more (Hesshaimer et al. 1994), were produced in the atmosphere. This artificial $^{14}C$ input caused a global increase in the $^{14}C/^{12}C$ ratio of atmospheric $CO_2$, leading to a substantial disequilibrium of $^{14}C$ between atmosphere, biosphere, and surface ocean water. In the decade following the testing, many laboratories from around the world conducted large observational programs to document stratospheric and tropospheric $^{14}CO_2$ changes as well as the penetration of bomb $^{14}C$ in all coupled reservoirs of the atmospheric carbon cycle. These measurements enable us to use $^{14}C$ as a unique tracer for carbon transfer processes between the reservoirs in question.

More than 30 years of direct tropospheric $^{14}CO_2$ observations from both hemispheres are now available since the nuclear test ban treaty in 1962 (Figure 2a) (Tans 1981; Nydal and Lövseth 1983; Levin et al. 1985, 1992; Manning et al. 1990; Meijer et al. 1995). Also, the stratosphere has been extensively sampled during and after the atmospheric bomb tests. The latter data were originally gathered by Telegadas (1971) who calculated bomb $^{14}C$ inventories for eight major sub-compartments of the stratosphere. A reassessment of the same data set was performed recently by Hesshaimer and Levin (2000), providing revised stratospheric inventories suitable for global carbon cycle and transport modeling (Figure 2b). The bomb $^{14}C$ decline observed in the troposphere mainly reflects the penetration of the $^{14}CO_2$ perturbation into the oceans and the biosphere, which is essentially driven by the internal circulation dynamics within each of these two reservoirs. But also, ongoing fossil fuel $CO_2$ emissions and $^{14}C$ sources such as nuclear facilities (Otlet et al. 1992, and references therein), and possibly nuclear underground detonations, contribute to the observed trend.

The oceans have been extensively sampled for $^{14}CO_2$ analysis in DIC during several international surveys: the Geochemical Ocean Sections Study (GEOSECS, 1972–1978), the Transient Tracers in the Ocean (TTO, 1980–1982) study, and the South Atlantic Ventilation Experiment (SAVE) are prominent examples in this context. In addition, the time development of $^{14}C$ in surface ocean water since preindustrial times, and including the bomb perturbation (Druffel and Suess 1983; Druffel 1995) was derived from corals that accrete annual density bands with $^{14}C$ activities equal to those of DIC in the surface water of the oceans (see Figure 2a). These data have been evaluated by Broecker et al. (1985, 1995) to determine the distribution of the natural $^{14}C$ component in DIC as well as the total bomb $^{14}C$ inventories of the world oceans. Their best figure of the global oceanic bomb $^{14}C$ inventory, normalized to 1 January 1974, amounts to $295 \pm 30 \times 10^{26}$ atoms of $^{14}C$ (Broecker et al. 1995) (see Figure 2b).

## Air–Sea Gas Exchange Rate and Internal Mixing of the Oceans

The combined analysis of the development of bomb $^{14}C$ in the global atmosphere as well as in the surface and deep oceans has given us insight into the strength of $CO_2$ exchange between the atmosphere and the oceans, as well as into the mixing dynamics within the oceanic reservoir itself. Accurate knowledge of these processes is crucial to determine the oceanic uptake of anthropogenic $CO_2$. The transport of excess $CO_2$ from the atmosphere into the interior of the oceans is limited by two kinds of transport resistance: air–sea gas exchange which is controlled by a thin water film at the water surface, and oceanic "mixing" circulation responsible for the exchange between the surface and deeper layers of the oceans. In many areas of the oceans, i.e. in mid-to-low latitudes, the gas exchange at the air–sea interface is fast enough, respectively, surface water renewal through mixing e.g. with the deep ocean is slow enough to ensure surface water to be almost in equilibrium with atmospheric $CO_2$ (the global mean equilibration time of ocean surface water is about 1 yr). However, in regions of the ocean with large deepwater formation rates, and respective fast renewal of the
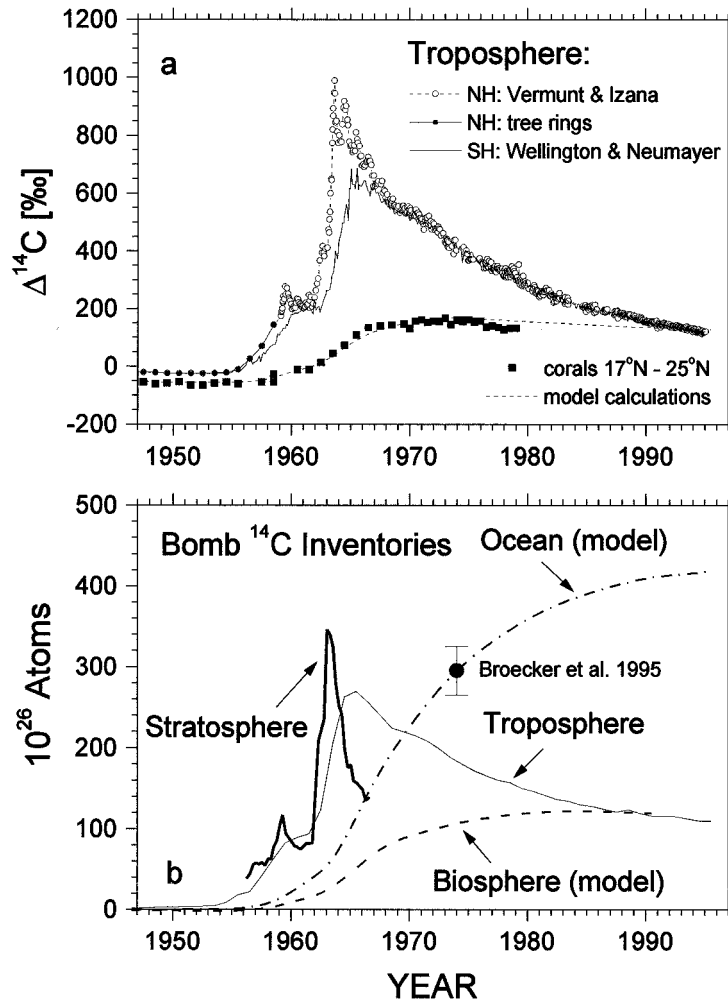
Figure 2  (a) Long-term observations of $\Delta^{14}C$ in atmospheric $CO_2$ in the northern and in the southern hemisphere (Manning et al. 1990; Levin et al. 1992 and unpublished Heidelberg data). Shortly after the atmospheric test ban treaty in 1962, the $^{14}CO_2$ level in the northern hemisphere was twice as high as the natural $^{14}CO_2$ level (defined as 0 in the $\Delta^{14}C$ scale [Stuiver and Polach 1977]). Also included is the $\Delta^{14}C$ level of DIC in surface ocean water between 17°N and 25°N derived from annual banded coral rings (Druffel and Suess 1983; Druffel 1995) together with model calculations for the surface ocean by Hesshaimer (1997). (b) Temporal trend of the observed bomb $^{14}C$ inventories of the stratosphere up to 30 km (Hesshaimer and Levin 2000), the troposphere (derived from the observations in [a]) the ocean (box-diffusion model estimates by Hesshaimer et al. [1994], tuned to fit the total inventory of Broecker et al. [1995]) and the biosphere (3-box compartment model estimates by Hesshaimer et al. [1994]).

surface water (i.e. in polar regions), the rate of gas exchange becomes important for net transport of excess $CO_2$ into the deep ocean (Siegenthaler 1983).

Both natural and bomb $^{14}C$ have been successfully used in the past to derive the mean atmosphere/ocean gas exchange rate for major ocean basins (Stuiver 1980; Stuiver et al. 1981). The net $^{14}C$ influx from the atmosphere to the surface ocean at a given time is proportional to the $\Delta^{14}C$ gradient

at the interface multiplied by the gross $CO_2$ exchange flux. In the undisturbed natural case, the global mean difference of $\Delta^{14}C$ between the atmosphere and the surface ocean was about 40‰. At equilibrium, the corresponding net $^{14}C$ influx was just enough to compensate the $^{14}C$ decay in the oceans, immediately yielding the $CO_2$ gas exchange flux for the preindustrial situation (ca. 280 ppm). During the period after 1955, disturbed by nuclear tests, the $CO_2$ gas exchange rate could be determined in an independent manner from the, in this case, time dependent uptake of bomb $^{14}C$ in the oceans until the time of GEOSECS (see Stuiver 1980). In this way, Stuiver et al. (1981) derived mean area-weighted $CO_2$ exchange fluxes for the Pacific and for the Atlantic oceans between 50°N and 50°S for 1955–1974. The bomb $^{14}C$-derived preindustrial gas exchange rate turned out to be in very good agreement with the mean steady state value. However, the $^{14}C$-derived gas exchange rates are larger by more than 30% if compared to figures derived from direct measurements in wind tunnels, over lakes and open ocean (Liss and Merlivat 1986; Boutin and Etcheto 1997). Although this discrepancy has not been fully resolved yet (Broecker et al. 1986; Wannikhof 1992), the $^{14}C$-derived exchange rate between the atmosphere and the ocean, leading to a gross exchange flux of about 90 GtC yr$^{-1}$ for the period 1980–1990 is adopted for all carbon-cycle models.

The dynamic model parameters for the internal mixing of the ocean have also been frequently determined by the distribution of natural $^{14}C$. Unfortunately, this procedure gives quite different answers for these fluxes than calibration with the bomb-$^{14}C$ distribution (Oeschger et al. 1975; Broecker et al. 1980; Siegenthaler 1983). The explanation for this discrepancy is that the distribution of natural $^{14}C$ is more sensitive to mixing processes on time scales of hundreds or thousands of years, whereas the characteristic time scale for the bomb $^{14}C$ uptake perturbation is only several decades. Siegenthaler and Joos (1992) solved this problem with their High-Latitude Exchange/Interior Diffusion-Advection (HILDA) model. They introduced an eddy diffusivity in the interior of the ocean, which is decreasing with depth. (In the original Oeschger-type box diffusion models, the eddy diffusivity is assumed constant with depth.) With this modification, natural *plus* bomb $^{14}C$-calibration yields a reliable description for the whole range of mixing processes in the ocean on all relevant time scales from 10 to 1000 yr. In particular, the calibration now provides a realistic description of the time-dependent uptake rates for anthropogenic excess $CO_2$ for the time scale in question, namely several hundred years.

### Budgeting Bomb $^{14}C$ in the Global Carbon Cycle

Natural and bomb $^{14}C$ have also been used in several studies to determine carbon turnover times within the terrestrial biosphere, in particular for SOM (e.g. Goudriaan 1992; Trumbore et al. 1993; Perruchoud et al. 1999). However, the heterogeneity of the terrestrial biosphere hampers the determination of globally valid bomb $^{14}C$ inventories for this reservoir based on observational data. Evidence on the exchange fluxes of bomb $^{14}CO_2$ with the biosphere is, however, also inherent to the *atmospheric* $^{14}CO_2$ record. It should, therefore, in principle be possible to gain insight into the cycling time of carbon *within* the biospheric reservoir by budgeting bomb $^{14}C$ in the global carbon system. This approach was used by Hesshaimer et al. (1994): The total decay-corrected bomb $^{14}C$ input into the carbon system at a given time must equal the sum of the corresponding bomb $^{14}C$ inventories of the stratosphere, the troposphere, the oceans, and the terrestrial biosphere. Besides the biospheric bomb $^{14}C$ inventory, the second unknown in this exercise is, however, the $^{14}C$ input from atmospheric bomb tests, i.e. the $^{14}C$ yield per Mt TNT. Theoretically, this $^{14}C$ yield can be derived from nuclear physics. However, those calculations have uncertainties in the order of nearly a factor of 2 (Bonka 1980; UNSCEAR 1982). The total bomb $^{14}C$ input into the atmosphere was, therefore, derived by Hesshaimer et al. (1994) on the basis of published bomb detonation strengths (Rath 1988) through adjusting the $^{14}C$ yield per Mt TNT to the tropospheric and stratospheric observations

during the time period of the major $^{14}CO_2$ rises (i.e. 1950–1963). As long as we trust the atmospheric observations and the bomb detonation strengths the uncertainty of this adjustment is small (in the order of about ±10%) since the total bomb $^{14}C$ uptake by the ocean and by the biosphere was not important before 1963.

A simple standard compartment model of the global carbon cycle (similar to the one by Oeschger et al. 1975) was then applied to infer the straight forward bomb $^{14}C$ budgeting. In doing so, Hesshaimer et al. (1994) found a serious mismatch in the total bomb $^{14}C$ inventory with an apparent $^{14}C$ source missing. Possible solutions for this mismatch have been argued to be due to: 1) an over-estimate of the oceanic bomb $^{14}C$ inventories, 2) residing bomb $^{14}C$ hot spots in the very high stratosphere, or 3) much less bomb $^{14}C$ uptake by the terrestrial biosphere than estimated from standard parameterizations of this reservoir (e.g. Goudriaan 1992). Other modeling studies, trying to globally match bomb $^{14}CO_2$ levels observed in the carbon cycle reservoirs (Enting et al. 1993; Broecker and Peng 1994; Lassey et al. 1996: Jain et al. 1997) solved inconsistencies in their budgets by generally mistrusting the stratospheric inventories of Telegadas (1971). These inventories have turned out to be largely confirmed by the revised calculations of Hesshaimer and Levin (2000) so that further investigations are necessary to solve the problem of budgeting bomb $^{14}C$ in the global carbon cycle. Solving this inconsistency, and in particular, independently confirming the penetration rate of bomb $^{14}C$ into the oceans, is crucial for the prediction of future atmospheric $CO_2$ concentrations because the oceanic uptake of excess $CO_2$ is generally normalized with bomb $^{14}C$ (see the Air–Sea Gas Exchange section above). As mentioned earlier, it is important to know *explicitly* which fraction of the anthropogenic emissions enters the biosphere and which fraction enters the oceans, because carbon storage in these two reservoirs behaves very differently. If the anthropogenic $CO_2$ is eventually stored in the deep oceans it is unlikely that it will re-enter the atmosphere within the next centuries. In contrast, $CO_2$ stored in the biosphere may be released back to the atmosphere within a few decades. Moreover, the capability of the terrestrial biosphere for uptake of excess-$CO_2$ is very sensitive to changes through human activities, in supply of nutrients and water, but also due to climatic feedback.

## Global Distribution of Atmospheric $^{14}CO_2$ in the 1990s and Beyond

The most prominent applications of the bomb $^{14}C$ perturbation as a transient tracer for carbon cycle studies took place in the 1970s and 1980s when the signal was largest in all reservoirs. After 1990, many of the extensive observational programs phased out as $^{14}CO_2$ approached a new quasi-natural equilibrium state. From 1982 onwards the globally decreasing $\Delta^{14}CO_2$ trend in fact almost exactly follows an exponential curve with a time constant of 18.70 ± 0.15 yr, thus changing from a decrease of about $\Delta^{14}CO_2 = -13‰$ yr$^{-1}$ in 1982 to about $-4‰$ yr$^{-1}$ in 1998 (see Figure 2a). With the last atmospheric bomb test being conducted in 1980, and although much weaker underground tests are still performed, bomb $^{14}C$ homogenized in the troposphere and additional input from the stratosphere became negligible. In the 1990s and today $^{14}CO_2$ in the troposphere, therefore, again reflects the distribution of natural and anthropogenic $CO_2$ sources and sinks. This is nicely illustrated by our modern high-precision measurements at seven globally distributed background stations located between 82°N (Alert, Nunavut, Canada) and 71°S (Neumayer, Antarctica) (Figure 3b). Although the north-south gradients are in the order of only a few per mil, a distinct structure is observed in the yearly mean $^{14}CO_2$ profile.

Figure 3b shows a relative $\Delta^{14}CO_2$ minimum in mid-northern latitudes. It is caused by the maximum effect of fossil fuel $CO_2$ emissions in this latitude belt. These anthropogenic emissions are also responsible for the north-south gradient of the $CO_2$ mixing ratio shown in Figure 3a, with about 1% higher concentrations in the northern than in the southern hemisphere. A second relative $\Delta^{14}CO_2$ minimum is observed in mid-to-high latitudes of the southern hemisphere and is associated with gas
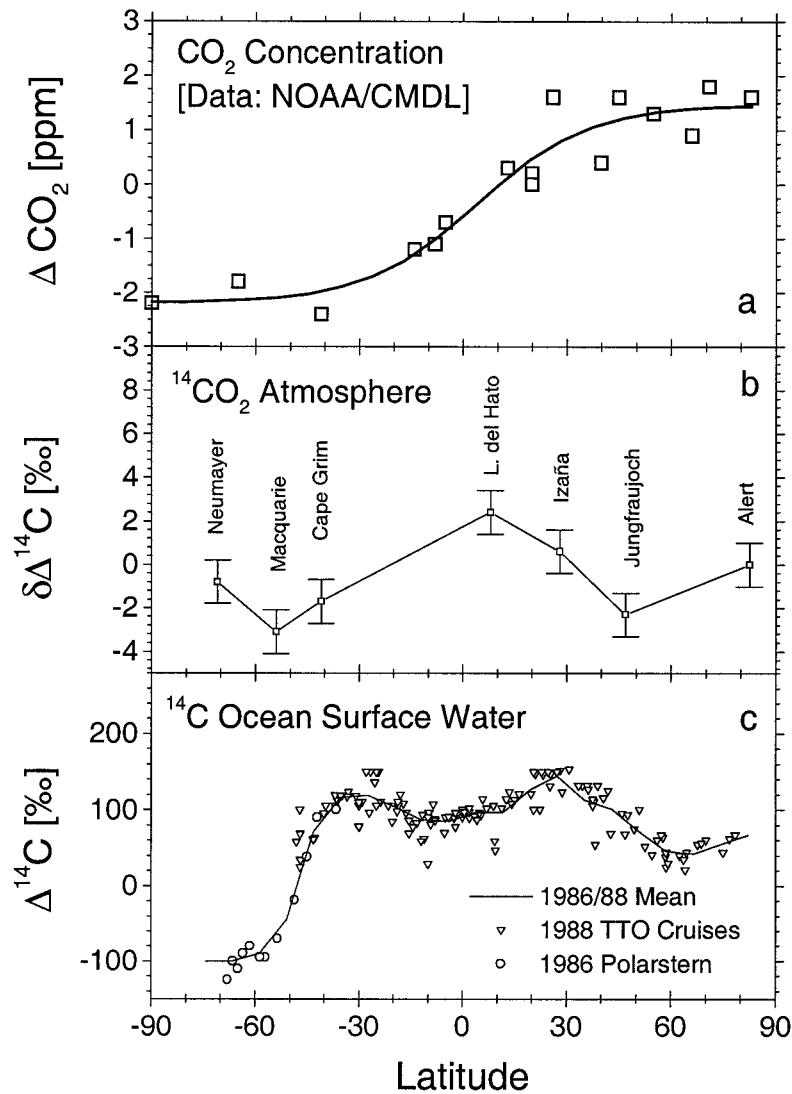
Figure 3  Mean meridional profiles 1993–1994 of (a) $CO_2$ concentration (data from the NOAA/ CMDL global network [Tans et al. 1996]) and (b) $\Delta^{14}CO_2$ in the atmosphere (Heidelberg unpublished data). Plotted are in (a) and (b) the deviations $\Delta CO_2$ and $\delta\Delta^{14}C$ from the global mean values. (c) $\Delta^{14}CO_2$ of DIC in surface ocean water derived from cruises of the TTO experiment (Broecker et al. 1995) together with unpublished Heidelberg data collected in 1986 in the South Atlantic ocean during the Polarstern cruise ANT III. The solid line represents a spline through the 1986/1988 data.

exchange with the circum Antarctic ocean surface: upwelling of intermediate water around Antarctica, which is depleted in $^{14}C$ (Figure 3c), causes a strong disequilibrium between atmospheric $^{14}CO_2$ and $^{14}C$ in DIC of the surface ocean water. The respective $CO_2$ flux from the ocean to the atmosphere is, therefore, depleted in $^{14}C$. Driven by the large *gross* exchange rate of $CO_2$ at these latitudes due to high wind speeds, a strong $^{14}C$ draw down is observed in the atmosphere at Macquarie Island and Neumayer. The two $\Delta^{14}C$ depleting effects in mid to high latitudes of both hemispheres cause a relative $\Delta^{14}CO_2$ maximum to appear in tropical and

subtropical regions (Figure 3b). This maximum is probably further enhanced by a net flux of bomb $^{14}C$ from the terrestrial biosphere to the atmosphere; two-thirds of the yearly terrestrial biospheric $CO_2$ exchange flux is located between 30°N and 30°S, the mean carbon turnover time of these ecosystems (i.e. tropical rain forests) being in the order of 30 yr. Bomb $^{14}C$ that was taken up in the early 1960s is now re-emitted to the atmosphere in the 1990s (see Figure 2b). This $^{14}C$ enriched biospheric $CO_2$ probably contributes to the $\Delta^{14}CO_2$ maximum observed at our tropical and subtropical sites. Although the $\Delta^{14}C$ signals in recent global background atmospheric $CO_2$ are rather small, they provide independent information on global $CO_2$ sources and sinks. This information has not yet been retrieved from the data sets by carbon-cycle modeling exercises.
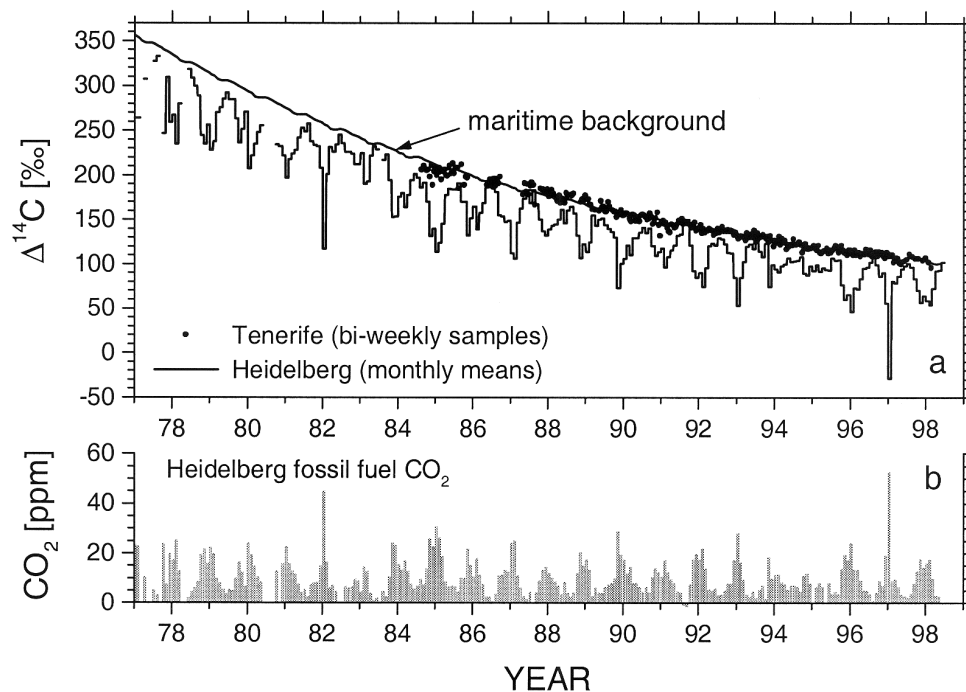


Figure 4 (a) Monthly mean $\Delta^{14}C$ observations in the upper Rhine valley at the polluted site Heidelberg together with the maritime background level, derived from observations at the baseline station Izaña, Tenerife (28°N) (Levin et al. 1989 and unpublished Heidelberg data). The maritime background $^{14}C$ level before 1988 is calculated from observations at Vermunt, Austria (47°N) (Levin et al. 1985), which were corrected by $\Delta^{14}C = +2‰$, therewith accounting for a general European fossil fuel offset. (b) Mean fossil fuel contribution at Heidelberg calculated with a two-component mixing model from the $\Delta^{14}C$ difference between Heidelberg and Izaña, the latter representing the maritime background level.

## Regional $^{14}C$ Suess Effect

As has been discussed above, the most important man-made perturbation of the atmospheric $CO_2$ cycle is the burning of fossil fuels, with about 95% of the $CO_2$ being released in the northern hemisphere. The fossil emissions today contribute about 50% to the decreasing $\Delta^{14}CO_2$ trend observed in the global atmosphere (Figure 2a). In polluted areas, e.g. over the European continent, an additional regional surplus of $CO_2$ from the burning of fossil fuels is clearly detectable as $\Delta^{14}C$ depletion relative to maritime levels. Levin et al. (1995) used $\Delta^{14}C$ observations to estimate the fossil fuel contribution to the continental $CO_2$ offset at Schauinsland station (Black Forest, Germany) to be around

1–3 ppm, depending on season. In more polluted areas, such as the upper Rhine valley in Heidelberg, the monthly mean fossil fuel contribution can be as large as several 10 ppm (Levin et al. 1989).

Figure 4a shows the updated $\Delta^{14}CO_2$ record for the Heidelberg site. Particularly during the winter months, mean $\Delta^{14}C$ depletions in the order of 50‰ are frequently observed. These translate into mean fossil fuel contributions of 20 ppm during this time of the year (Figure 4b). In fact, during summer, the fossil fuel contributions are generally expected to be much lower due to enhanced vertical mixing and dilution of ground-level pollutants but also due to reduced emissions (no domestic heating). The interannual changes of the yearly mean regional fossil fuel contributions are small, however, and a general trend, i.e. towards decreasing offsets, cannot be detected in the last 20 years. In fact, from statistical emissions data of southern Germany no significant trend should be expected from 1987 to 1996. The mean values for the five-year periods from 1987 to 1991 (8.98 ± 0.31 ppm) and from 1992 to 1996 (8.90 ± 0.58 ppm) compare extremely well within ±1%. This opens the possibility of using regional $\Delta^{14}C$ observations to validate fossil fuel emissions reductions, e.g. in the frame of the Kyoto Protocol; here, Germany and the European Union as a whole are obliged to reduce their emissions of $CO_2$ and other greenhouse gases by 8% by 2008–2012, a reduction that will be clearly visible and quantifiable using our $^{14}C$-based regional observations in the time frame of a five-year period.

## CONCLUSION

The radioactive lifetime of $^{14}C$ is perfectly suited for dating of carbon pools interacting with the atmospheric $CO_2$ reservoir on the time scale of several hundred to several thousand years. The above examples clearly show that our quantitative knowledge of the present gross and net fluxes of $CO_2$ between the dominant carbon reservoirs is significantly based on respective information provided through radiocarbon observations. In particular the use of bomb $^{14}C$ as a transient tracer in the carbon system provides invaluable insight into processes on the time scale where the largest man made $CO_2$ perturbations took place, namely the last 50–100 yr. The most prominent example is the air–sea gas exchange and the penetration of human $CO_2$ disturbances from the surface into deeper layers of the oceans. Finally, the unique characteristics of fossil fuel derived $CO_2$ being $^{14}C$-free allows the tracking of respective emission changes in the past and also in coming years when reliable tools are needed to validate national emission claims of greenhouse gases in the frame of the Kyoto negotiations.

## REFERENCES

Bonka H. 1980. Produktion und Freisetzung von Tritium und Kohlenstoff-14 durch Kernwaffenversuche, Testexplosionen und kerntechnische Anlagen, einschließlich Wiederaufarbeitungsanlagen. In: Stieve FE, Kirstner G, editors. *Strahlenschutzprobleme im Zusammenhang mit der Verwendung von Tritium und Kohlenstoff-14 und ihren Verbindungen.* Berlin: Dietrich Reimer Verlag. p 17–26.

Boutin J, Etcheto J. 1997. Long-term variability of the air-sea $CO_2$ exchange coefficient: consequences for the $CO_2$ fluxes in the equatorial Pacific Ocean. *Global Biogeochemical Cycles* 11:453–70.

Broecker WS, Peng T-H. 1994. Stratospheric contribution to the global bomb radiocarbon inventory: model versus observation. *Global Biogeochemical Cycles* 8(3):377–84.

Broecker WS, Peng T-H, Engh R. 1980. Modelling the carbon systen. *Radiocarbon* 22(3):565–98.

Broecker WS, Peng T-H, Östlund G, Stuiver M. 1985. The distribution of bomb radiocarbon in the ocean. *Journal of Geophysical Research* 90:6953–70.

Broecker WS, Ledwell JR, Takahashi T, Weiss R, Merlivat L, Memery L, Peng T-H, Jähne B, Münnich KO. 1986. Isotopic versus micrometeorological ocean $CO_2$ fluxes: a serious conflict. *Journal of Geophysical Research* 91(C9):10,517–27.

Broecker WS, Sutherland S, Smethie W, Peng T-H, Östlund G. 1995. Oceanic radiocarbon: Separation of the natural and bomb components. *Global Biogeochemical Cycles* 9(2):263–88.

Conway TJ, Tans PP, Waterman LS, Thoning KW, Kitzis DR, Masarie KA, Zhang N. 1994. Evidence for inter-

annual variability of the carbon cycle from the NOAA/CMDL global air sampling network. *Journal of Geophysical Research* 99:22,831–55.

De Jong AFM, Mook WG. 1982. An anomalous Suess effect above Europe. *Nature* 298:1–3.

Druffel EM, Suess HE. 1983. On the radiocarbon record in banded corals: exchange parameters and net transport of $^{14}CO_2$ between atmosphere and surface ocean. *Journal of Geophysical Research* 88(C2):1271–80.

Druffel EM. 1995. Pacific bomb radiocarbon coral data. In: *IGBP PAGES/World Data Center-A for Paleoclimatology*. Boulder: NOAA/NGDC Paleoclimatology Program.

Enting IG, Lassey KR, Houghton RA. 1993. Projections of future $CO_2$. CSIRO DAT Technical Paper 27. Division of Atmospheric Research, Commonwealth Science and Industry Research Organization. Mordialloc, Australia.

Etheridge DM, Steele LP, Francey RJ, Langenfels RL. 1996. Natural and anthropogenic changes in atmospheric $CO_2$ over the last 1000 years from air in Antarctic ice and firn. *Journal of Geophysical Research* 101(D2):4115–28.

Goudriaan J. 1992. Biosphere structure, carbon sequestering potential and the atmospheric $^{14}C$ carbon record. *Journal of Experimental Botany* 43:1111–9.

Hesshaimer V. 1997. Tracing the global carbon cycle with bomb radiocarbon. PhD dissertation. University of Heidelberg.

Hesshaimer V, Levin I. 2000. Revision of the stratospheric bomb $^{14}C$ inventory. *Journal of Geophysical Research*. Forthcoming.

Hesshaimer V, Heimann M, Levin I. 1994. Radiocarbon evidence for a smaller oceanic carbon dioxide sink than previously believed. *Nature* 370:201–3.

Jain AK, Kheshgi HS, Wuebbles DJ. 1997. Is there an imbalance in the global budget of bomb-produced radiocarbon? *Journal of Geophysical Research* 102(D1):1327–33.

Keeling CD, Worf TP. 1999. Atmospheric $CO_2$ concentration derived from in situ air samples collected at Mauna Loa Observatory, Hawaii. *CDIAC WDC-A database*, Oak Ridge National Laboratory. Http://cdiac.esd.ornl.gov/ftp/ndp001/.

Lassey KR, Enting DJ, Trudinger CM. 1996. The earth's radiocarbon budget – a consistent model of the global carbon and radiocarbon cycles. *Tellus* 48B:487–501.

Levin I, Kromer B. 1997. Twenty years of atmospheric $^{14}CO_2$ observations at Schauinsland station, Germany. *Radiocarbon* 39(2):205–18.

Levin I, Kromer B, Schoch-Fischer H, Bruns M, Münnich M, Berdau B, Vogel JC, Münnich KO. 1985. 25 years of tropospheric $^{14}C$ observations in central Europe. *Radiocarbon* 27(1):1–19.

Levin I, Schuchard J, Kromer B, Münnich KO. 1989. The continental European Suess effect. *Radiocarbon* 31(3):431–40.

Levin I, Bösinger R, Bonani G, Francey R, Kromer B, Münnich KO, Suter M, Trivett NBA, Wölfli W. 1992. Radiocarbon in atmospheric carbon dioxide and methane: global distribution and trends. In: Taylor RE, Long A, Kra R, editors. *Radiocarbon after four decades: an interdisciplinary perspective*. New York: Springer-Verlag. p 503–18.

Levin I, Graul R, Trivett NBA. 1995. Long term observations of atmospheric $CO_2$ and carbon isotopes at continental sites in Germany. *Tellus* 47B:23–34.

Liss PS, Merlivat L. 1986. Air-sea gas exchange rates: Introduction and synthesis. In: Buat-Menard P, editor. *The role of air-sea exchange in geochemical cycling*. Hingham, Massachusetts: D Reidel. 113–27.

Manning MR, Lowe CM, Melhuish WH, Sparks RJ, Wallace G, Brenninkmeijer CAM, McGill RC. 1990. The use of radiocarbon measurements in atmospheric studies. *Radiocarbon* 32(1):37–58.

Marland G, Boden T, Brenkert A, Johnston C. 1999. Global, regional and national $CO_2$ emission estimates from fossil fuel burning, cement production, and gas flaring: 1751–1996. CDIAC WDC-A database, Oak Ridge National Laboratory. Http://cdiac.ornl.gov/ndps/ndp030.html.

Meijer HAJ, Van der Plicht J, Gislefoss JS, Nydal R. 1995. Comparing long term atmospheric $^{14}C$ and $^{3}H$ records near Groningen, the Netherlands with Fruholmen, Norway and Izana, Canary Islands $^{14}C$ stations. *Radiocarbon* 37(1):39–50.

Neftel A, Moor E, Oeschger H, Stauffer B. 1985. Evidence from polar ice cores for the increase in atmospheric $CO_2$ in the past two centuries. *Nature* 315:45–7.

Nydal R, Lövseth K. 1983. Tracing bomb $^{14}C$ in the atmosphere 1962–1980. *Journal of Geophysical Research* 88(C6):3621–42.

Oeschger H, Siegenthaler U, Schotterer U, Gugelmann A. 1975. A box diffusion model to study the carbon dioxide exchange in nature. *Tellus* 27:168–192.

Otlet RL, Fulker MJ, Walker AJ. 1992. Environmental impact of atmospheric Carbon-14 emissions resulting from the nuclear energy cycle. In: Taylor RE, Long A, Kra R, editors. *Radiocarbon after four decades: an interdisciplinary perspective*. New York: Springer-Verlag. p 519–34.

Perruchoud D, Joos F, Fischlin A, Hajdas I, Bonani G. 1999. Evaluating time scales of carbon turnover in temperate forest soils with radiocarbon data. *Global Biogeochemical Cycles* 13:555–73.

Rath HK. 1988. Simulation der globalen $^{85}Kr$ und $^{14}CO_2$ Verteilung mit Hilfe eines zeitabhängigen, zweidimensionalen Modells der Atmosphäre [PhD dissertation]. Universität Heidelberg.

Schimel D, Enting I, Heimann M, Wigley T, Raynaud D, Alves D, Siegenthaler U. 1995. The global carbon cycle. In: Houghton J et al., editors. *Climate change 1994: radiative forcing of climate change and an eval-*

uation of the IPCC IS92 emission scenarios. Cambridge: Cambridge University Press. p 35–71.

Siegenthaler U. 1983. Uptake of excess $CO_2$ by an outcrop-diffusion model of the ocean. *Journal of Geophysical Research* 88(C6):3599–3619.

Siegenthaler U, Joos F. 1992. Use of a simple model for studying oceanic tracer distributions and the global carbon cycle. *Tellus* 44B(3):186–207.

Siegenthaler U, Sarmiento JL. 1993. Atmospheric carbon dioxide and the ocean. *Nature* 365:119–25.

Stuiver M. 1980. [14]C distribution in the Atlantic Ocean. *Journal of Geophysical Research* 85:2711–8.

Stuiver M, Polach H. 1977. Discussion: reporting of ^{14}C data. *Radiocarbon* 19(3):355–63.

Stuiver M, Quay P. 1981. Atmospheric ^{14}C changes resulting from fossil fuel $CO_2$ release and cosmic ray flux variability. *Earth and Planetary Science Letters* 53:349–62.

Stuiver M, Oestlund HG, McConnaughey TA. 1981. GEOSECS Atlantic and Pacific ^{14}C distribution. In: Bolin B, editor. *SCOPE 16, carbon cycle modelling*. Chichester, New York, Brisbane, Toronto: Wiley. p 201–21.

Suess HE. 1955. Radiocarbon concentration in modern wood. *Science* 122:415.

Tans PP, De Jong AFM, Mook WG. 1979. Natural atmospheric ^{14}C variation and the Suess effect. *Nature* 280: 826–7.

Tans PP. 1981. A compilation of bomb ^{14}C data for use in global carbon model calculations. In: Bolin B, editor. *SCOPE 16, carbon cycle modelling*. Chichester, New York, Brisbane, Toronto: Wiley. p 131–57.

Tans PP et al. 1996. Carbon cycle. In: Hofmann DJ, Peterson JT, Rosson RM, editors. *Summary report 1994–1995, Climate Monitoring and Diagnostics Laboratory No. 23*. NOAA: DOE. p 29–49.

Telegadas K. 1971. The seasonal atmospheric distribution and inventories of excess carbon-14 from March 1955 to July 1969. *Report HASL* 243:12–187 (avail. NTIS, Springfield, Virginia 22151).

Trumbore SE. 1993. Comparison of carbon dynamics in temperate and tropical soils. *Global Biogeochemical Cycles* 7:275–90.

UNSCEAR. 1982. Report to the General Assembly, ionising radiation: sources and biological effects. New York: UNO.

Wanninkhof R. 1992. Relationship between wind speed and gas exchange over the ocean. *Journal of Geophysical Research* 97:7373–82.